Carbohydrate Polymers 92 (2013) 1579–1585

Contents lists available at SciVerse ScienceDirect

Carbohydrate Polymers

journal homepage: www.elsevier.com/locate/carbpol

Biodegradable multilayer barrier films based on alginate/polyethyleneimine and biaxially oriented poly(lactic acid)

Chun-Hong Gu [a], Jia-Jun Wang [a,b,*], Yang Yu [a], Hui Sun [a], Ning Shuai [a], Bing Wei [a]

[a] College of Materials and Textiles, Zhejiang Sci-Tech University, Hangzhou 310018, China
[b] Key Laboratory of Advanced Textile Materials and Manufacturing Technology, Ministry of Education of China, Zhejiang Sci-Tech University, Hangzhou 310018, China

ARTICLE INFO

Article history:
Received 27 July 2012
Received in revised form 27 October 2012
Accepted 1 November 2012
Available online 10 November 2012

Keywords:
Biaxially oriented poly(lactic acid) (BOPLA)
Layer-by-layer (LBL)
Oxygen permeability
Permeation mechanism
Film properties

ABSTRACT

A layer-by-layer (LBL) approach was used to assemble alternating layers of sodium alginate (ALG)/polyethyleneimine (PEI) on biaxially oriented poly(lactic acid) (BOPLA) films in order to produce bio-based all-polymer thin films with low gas permeability. Increasing the depositing of ALG and PEI from 0 to 30 layers results in large thickness variations (from 0 to 3.92 μm). After 30 ALG/PEI layers are deposited, the resulting assembly has an OTR of 1.22 $cm^3/(m^2$ day atm). When multiplied by thickness, the resulting oxygen permeability (OP) is found to be less than 3.8×10^{-17} cm^3 cm/cm^2 s Pa, which is almost 3 orders of magnitude lower than that of uncoated BOPLA film (1.8×10^{-14} cm^3 cm/cm^2 s Pa). At the same time, the resulting multilayer-coated BOPLA films maintain high optical clarity and tensile properties. This unique barrier thin film has become a promising alternative to non-biodegradable synthetic food packaging materials.

1. Introduction

The growth of environmental problems and exhausting natural resources caused by non-biodegradable petrochemical-based packaging materials has raised a renewed interest in developing biodegradable materials (Liu & Berglund, 2012). The results suggest that polymers derived from renewable sources have the potential to be used as alternatives to petroleum based polymers in packaging applications (Picard, Espuche, & Fulchiron, 2011; Vartiainen, Tammelin, Pere, Tapper, & Harlin, 2010). Among the renewable source-based biodegradable plastics, poly(lactic acid) (PLA) film is one of the most promising materials since it can achieve excellent mechanical properties, biodegradability and biocompatibility (Fortunati et al., 2012; Rhim, Hong, & Ha, 2009; Yu et al., 2012). However, compared with the conventional non-biodegradable polymer resins, PLA exhibits low resistance to oxygen and water vapor permeation (Delpouve, Stoclet, Saiter, Dargent, & Marais, 2012; Jamshidian et al., 2012; Marais, Kochumalayil, Nilsson, Fogelstrom, & Gamstedt, 2012). Therefore, many studies have focused on improving the gas barrier properties of PLA by different modified methods, such as the incorporation of other nano-scale materials (Rhim et al., 2009; Sanchez-Garcia & Lagaron, 2010), organic–inorganic hybrid coatings (Bang & Kim, 2012; Iotti, Fabbri, Messori, Pilati, & Fava, 2009; Park et al., 2012) and the lamination of other polymers (Cho, Gallstedt, & Hedenqvist, 2010).

Recently, a developed alternative strategy using a bottom-up layer-by-layer (LBL) process has been employed as a powerful way to assemble gas barrier multilayer thin films by sequential adsorption of oppositely charged polyelectrolytes or particles (Koch, Akhave & Bharadwaj, 2003), as shown in Fig. 1. The LBL technique presents a great advantage over many other coating techniques in that the coatings of nanometer-thickness can be tailorable simply by adjusting some factors such as the deposition pH and the number of dipping cycles (Guzman et al., 2011; Priolo, Gamboa, & Grunlan, 2010). From the perspective of packaging applications, LBL assembly films can be made to exhibit flame retardant behavior (Li et al., 2010), super mechanical properties (Podsiadlo, Tang, Shim, & Kotov, 2007; Sui, Huang, Podsiadlo, Kotov, & Kieffer, 2010), antimicrobial behavior (Dvoracek, Sukhonosova, Benedik, & Grunlan, 2009) and gas barrier properties (Jang, Rawson, & Grunlan, 2008). LBL technique has been used to create multilayer coatings consisting of negatively charged clay and cationic polymer on a poly(ethylene terephthalate) (PET) substrate resulting oxygen barrier dramatically increased (Priolo, Gamboa, Holder, & Grunlan, 2010). More recently, this concept has been applied to clay–biopolymer assemblies on biodegradable PLA films that exhibits high oxygen barrier (Laufer, Kirkland, Cain, & Grunlan, 2012; Svagan et al., 2012). These environmental benign nanocoated PLA films can be developed as an ideal candidate for food packaging to be competitive with the synthetic plastics (e.g., PET).

* Corresponding author at: College of Materials and Textiles, Zhejiang Sci-Tech University, Hangzhou 310018, China. Tel.: +86 13357189963; fax: +86 057186843255.
E-mail address: pelzstu@yahoo.cn (J.-J. Wang).

0144-8617/$ – see front matter © 2012 Elsevier Ltd. All rights reserved.
http://dx.doi.org/10.1016/j.carbpol.2012.11.004

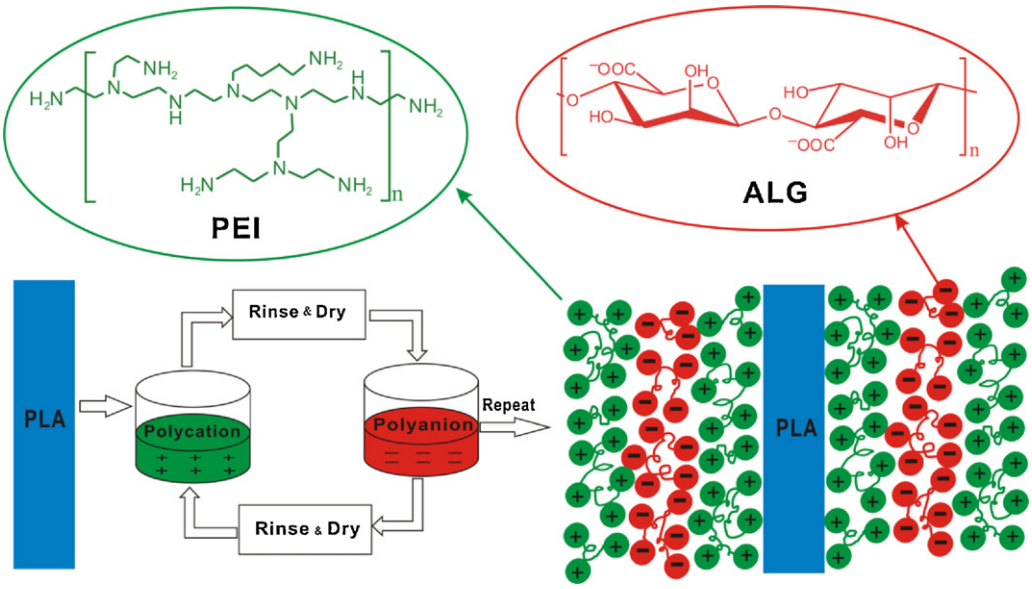

Fig. 1. Schematic of the LBL deposition process and a simplified image of the resulting multilayer ALG/PEI structure deposited on the BOPLA films.

New biodegradable all-polymer multilayer coatings have been deposited via LBL technique to impart mechanical properties (De Mesquita, Donnici, & Pereira, 2010; Rossier-Miranda, Schroen, & Boom, 2010), biocompatibility (Xie, Wang, & Yao, 2009), antifog properties (Nuraje, Asmatulu, Cohen, & Rubner, 2011). To our knowledge, there are only a few publications on the gas barrier properties of all-polymer multilayer films on PET (Carneiro-Da-Cunha et al., 2010; Yang, Haile, Park, Malek, & Grunlan, 2011). These coated PET films may, however, not be ideal for biodegradable food packaging applications because they are either nonbiodegradable or possessing relatively low barrier properties. Earlier investigations have indicated that it is possible to assemble cationic polyelectrolytes and natural polysaccharides to form multilayers on the biodegradable substrate (e.g., PLA) in biomedical engineering (Zhu, Gao, He, Liu, & Shen, 2003; Zhu, Ji, Tan, Barbosa, & Shen, 2003). The build-up of multilayers using all-polymer biodegradable polymers may also be applied to food packaging field, and to the best of our knowledge, multilayer build-up of both oxygen and water vapor barrier films using biomaterials on biodegradable BOPLA has not previously been reported.

In our work, novel biodegradable all-polymer multilayer-coated BOPLA films are constructed through LBL technique to improve the oxygen barrier of the BOPLA film significantly. Water vapor barrier properties, mechanical properties and transparency are also researched, which will assist in competing with non-biodegradable plastic (e.g., PE, PET) in food packaging application.

2. Experimental

2.1. Materials

Sodium alginate (ALG, at 0.2 wt%, pH = 7) was purchased from Sinopharm Chemical Reagent Co., Ltd. (China). Chitosan (CS) with a degree of deacetylation of 90% (viscosity = 152 mPa s at 0.2 wt%, w/w, in 3%, v/v, acetic acid solution with a pH of 3) was supplied by Golden-Shell Biochemical Co., Ltd. (China). Branched polyethylenimine (PEI) (Mw = 10,000 g/mol) was purchased from Aladdin chemistry Co., Ltd., China and dissolved into distilled water to create a 0.1 wt% solution (pH = 9.5). The pH was adjusted using 1 mol/L sodium hydroxide or 1 mol/L hydrochloric acid solution, respectively. The BOPLA films were provided by Shenzhen Esun Industrial Co., Ltd., China. The films had a thickness of 27 μm, a typical film thickness used in the production of packaging bag for food packaging.

2.2. Preparation of multilayers on BOPLA

The overall multilayer assembly process is shown in Fig. 1. Prior to LBL assembly, each BOPLA film of 10 cm × 10 cm piece, rinsed with ethanol/water (1:1, v/v) solution for 2 h, followed by a thorough rinsing with distilled water (pH = 7), was immersed in PEI solution for 3 h at room temperature, and then washed with a large amount of distilled water. The aminolyzed BOPLA films were treated with HCl (pH = 4) solution for 3 min at room temperature and then washed with a large amount of distilled water, and dried to constant weight. The modified BOPLA substrate was initially dipped into the polyanion (ALG) solution for 5 min. Then the substrate was rinsed with distilled water for 3 min and dried with blowing air. After the first layer of negatively charged polymer was adsorbed, the substrate was dipped into the polycation (PEI or CS) solution for another 5 min followed by another rinsing and drying cycle. The above procedure was repeated for subsequent layers using 5 min dip times until the desired number of layers was achieved. All coated films were dried at 30 °C under reduced pressure prior to characterization.

2.3. Film growth

Contact angles of the nanocoated film surface were measured by a video contact angle meter (OCA-20, Kruss, Germany) using the sessile drop method. A 3 μL droplet of MilliQ water was placed on the horizontal surface with a 50 μL glass syringe. Measurements were made at equilibrium after drop deposition and duplicate measurements were performed on three different areas of each sample at room temperature (25 °C). The UV–vis analyses were performed using a UV-vis spectrophotometer (Jasco 560, Germany) and were used to follow the multilayer films construction. The absorbance was measured at 260 nm on dried films.

2.4. Film properties

The oxygen transmission rate (OTR, $cm^3/(m^2\ day\ atm)$) values were performed with a VAC-V_1 gas permeability tester (Labthink Instruments Co., Ltd., China). The tests were carried out at 23 °C, and

50% RH. Two specimens were tested for each film type. The water vapor transmission rate (WVTR g/(m^2 24)) values were measured gravimetrically using a TSY-T_3 WVP tester (Labthink Instruments Co., Ltd., China). Tests were performed at 38 ± 0.2 °C and 90% RH. Two specimens were tested for each film type. The OP coefficients and the WVP were calculated using Eq. (1).

$$QP = \frac{QTR \cdot t}{\Delta p} \quad (1)$$

In Eq. (1), QP is the gas permeability coefficient (OP, cm^3 cm/cm^2 s Pa) or gas permeability coefficient (WVP, g cm/cm^2 s Pa), QTR is the oxygen transmission rate (OTR) or the water vapor transmission rate (WVTR), Δp is the partial pressure of the water on the two sides of the film, and t is the sample thickness. For the tensile tests, film specimens were cut into rectangular shapes that were 1.5 cm wide and 10 cm long. Tensile properties, such as tensile strength (TS) and elongation at break (%*E*) of each BOPLA and coated-BOPLA films, were evaluated with a XLW auto tensile tester (Labthink Instruments Co., Ltd., China). Samples were conditioned for 48 h at 23 °C and 50% RH in a constant temperature and humidity chamber before the measurement. The initial grip separation and the crosshead speed were set at 50 mm and 50 mm/min, respectively. Tensile strength and elongation at break were calculated by five replicates. Transparency was determined using a WGT-S light transmittance and haze tester (INESA Instruments Co., Ltd., China).

2.5. Morphology of multilayer-coated BOPLA films

AFM images of the surface structure of the coated BOPLA films were imaged in tapping mode under ambient air conditions (23 °C and 50% RH) using a XE-100E atomic force microscope (Park System, Korea). FESEM analyses were performed with ULTRA-55 electron microscope (Carl Zeiss SMT Pte Ltd., Germany). Before analysis, all samples were broken in liquid nitrogen and mounted on aluminum stubs using carbon adhesive tape.

2.6. Statistical analysis

Microsoft Excel-2003 was used for all statistical analyses. The data were determined by the analysis of variance (ANOVA), and the means were compared using Student's *t*-test. Significance was defined at a level of $P < 0.05$.

3. Results and discussion

3.1. Film growth

3.1.1. Contact angle

The contact angles of the alternate deposition of oppositely charged polyelectrolytes can be observed in Fig. 2A. Samples with an odd number of layers have ALG as the outermost layer, whereas samples with an even number of layers have CS or PEI as the outermost layer excepting samples of BOPLA virgin substrate as layer zero. It could be seen that the contact angles of the odd deposited layers (ALG as the outermost layer) were higher than the even layers (CS/PEI as the outermost layer). The successful assembly of the polyelectrolytes on BOPLA films was verified by the change of contact angles alternating. In both ALG/PEI and ALG/CS system, it was observed that contact angles of the alternate assembling polycation layers were higher than polyanion layers, illustrating that ALG is more hydrophilic than both PEI and CS (Lawrie et al., 2007; Zhu, Ji, & Shen, 2004). Comparing the polycation layers, the contact angles of adsorbed PEI layers were much higher than adsorbed CS layers, which implied a more hydrophobic structure of PEI layers than the resulting CS layers.

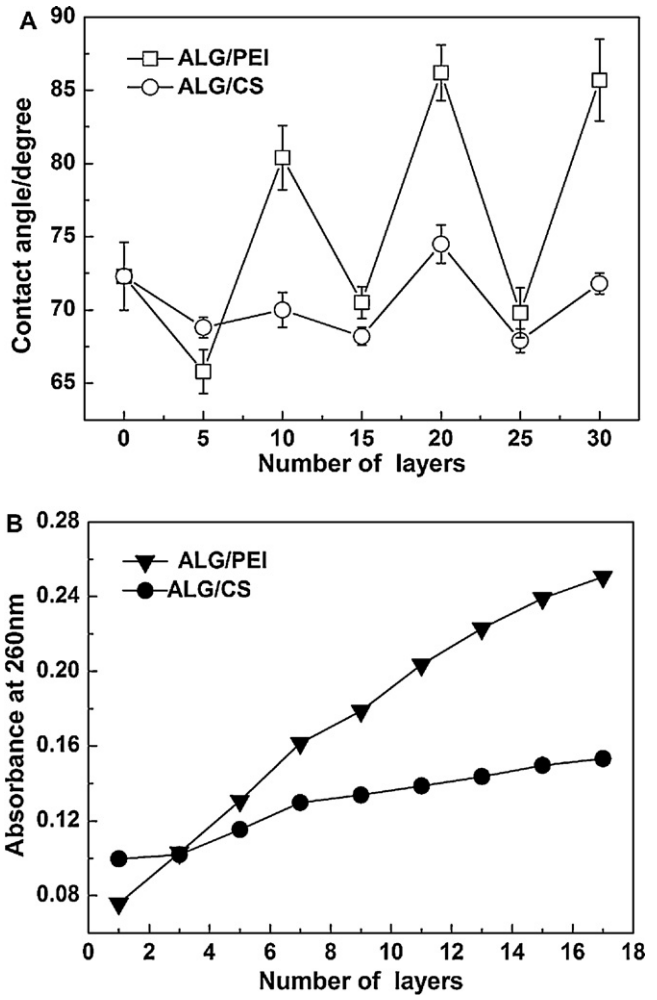

Fig. 2. Contact angle data of the alternate deposition of ALG and CS (PEI) and UV–vis absorbance at 260 nm of the assembled ALG layers on the BOPLA substrate are shown in (A) and (B), respectively.

3.1.2. UV–vis spectral analysis

The successful buildup of the ALG/PEI and ALG/CS layers on the BOPLA matrix in the cyclic dipping procedure can be visualized by UV–visible spectroscopy at 260 nm (Carneiro-Da-Cunha et al., 2010; Wasikiewicz, Yoshii, Nagasawa, Wach, & Mitomo, 2005). As shown in Fig. 2B, the absorbance at 260 nm of the UV–vis spectra showed a linear increase with the increase of ALG/PEI bilayers, which was typical for many LBL assembled pairs. It suggested that the thickness of every new ALG/PEI bilayer increased linearly with the increase of the layers. However, in Fig. 2B, the intensity of the absorbance increased irregularly with the growth of ALG/CS before the first four or five layers. After that, it showed a linear increase of absorbance with more ALG adsorption. After that, it showed a linear increase of absorbance with more ALG adsorption. Similar film growth behavior has been observed with other polysaccharide multilayers, which comprised of two distinct stages. The first stage is characterized by isolated island growth, whereas the second stage involves a more continuous film construction (Nuraje et al., 2011; Richert et al., 2004). Moreover, compared with the absorbance of ALG/CS system (from about 0.09969 to 0.15331), the absorbance of ALG/PEI system showed a relatively broader range (from about 0.0758 to 0.2506) when 17 layers were deposited. This implied a thicker assembling of ALG/PEI than that of ALG/CS on BOPLA films. This is in accordance with the thickness of ALG/PEI layer and ALG/CS layer that we have measured in Fig. 3.

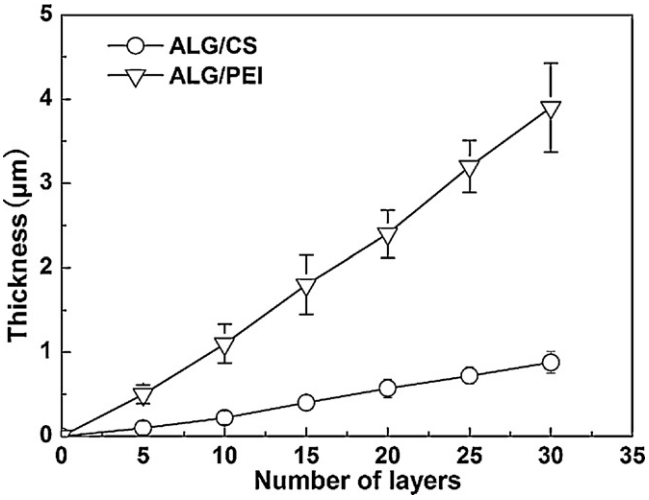

Fig. 3. Film thickness as a function of the number of layers deposited.

3.2. Film properties

3.2.1. Oxygen and water vapor permeability

As to ALG/PEI alternately coated system, the oxygen barrier properties, which are largely improved with the numbers of assembling layers increased from 0 to 30, are presented in Fig. 4. The OTR of neat BOPLA and multilayer-coated BOPLA film is shown in Fig. 4A. In this case, with the layers of ALG/PEI increased to 30 layers, the reported OTR values decrease by 99.8% compared with the pure BOPLA (580 $cm^3/(m^2$ day atm)). This super oxygen barrier is comparable to multilayer coatings consisting of PAA/PEI prepared by Grunlan et al. (Yang et al., 2011). As a result, the multilayer-coated BOPLA film containing polysaccharides can reduce the oxygen permeability to a great extent in spite of the hydrophilic nature. As shown in Fig. 4B, the oxygen permeability coefficients (OP) data of the total film (LBL coating and BOPLA film together) is presented in order to eliminate the effect of the film thickness. These data were calculated from the reported OTR in Fig. 4A using Eq. (1). The OP of the uncoated BOPLA film is 1.8125×10^{-14} cm^3 cm/cm^2 s Pa, which is in agreement with reported values for PLA films of similar compositions (Laufer et al., 2012; Sanchez-Garcia & Lagaron, 2010). The OP of 10 layer coated BOPLA film decreased to 1.037×10^{-15} cm^3 cm/cm^2 s Pa, which is still more than 1 order of magnitude lower than that of neat BOPLA film. As a result, the oxygen permeability of BOPLA film coated with 10 layers of ALG/PEI is equivalent to that of bare PET film (Priolo, Holder, Gamboa, & Grunlan, 2011), which is considered to be a good barrier to oxygen. The 30 layer coated BOPLA thin film exhibits the lowest oxygen permeability (3.851×10^{-17} cm^3 cm/cm^2 s Pa) that is almost 3 orders of magnitude lower than that of uncoated BOPLA film. Fig. 4A also shows the thin film permeability as a function of layers of these coatings. The coating oxygen permeability is obtained by decoupling from the total film permeability (OP) using a previously described method (Roberts et al., 2002). The thin film permeability exhibited by this 30 layer coating is the lowest ever reported for a biodegradable all-polymer LBL assembly (4.8×10^{-18} cm^3 cm/cm^2 s Pa). The significantly increased barrier properties in this study may stir up further research in barrier films based on carbohydrate polymers.

The enhanced oxygen barrier may presumably link to the opposite charge overcompensation during the adsorption step leading to a highly interpenetrating polymeric network, which could reduce free volume for the interfacial polymer (Yang et al., 2011; Zhang & Peppas, 2000). Other than the interpenetrating effects, polymer chains are confined to a smaller volume through

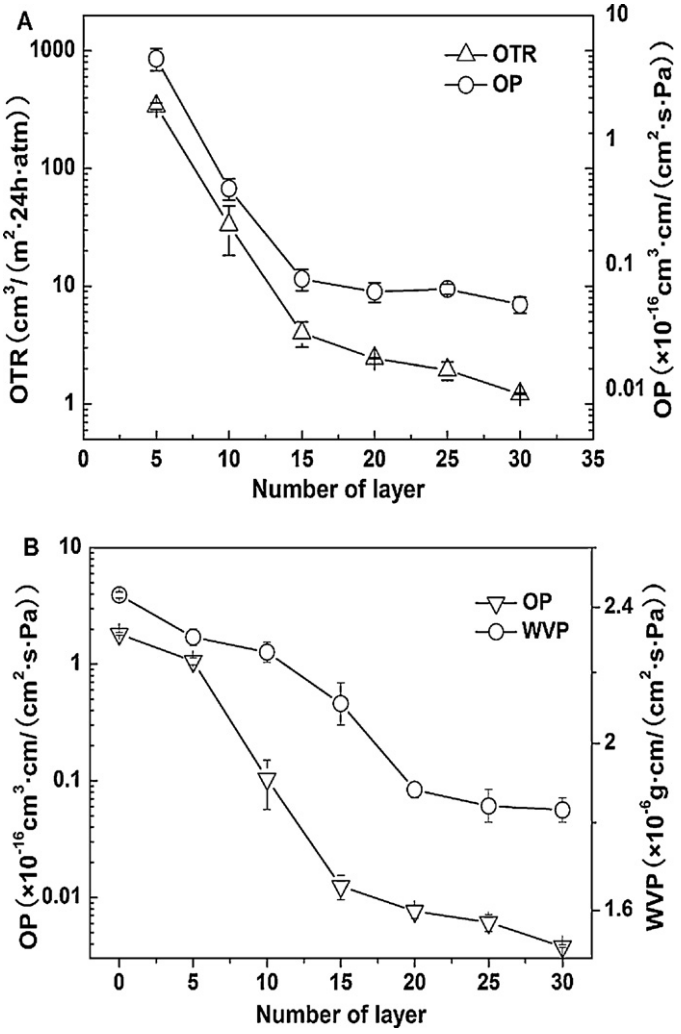

Fig. 4. (A) Oxygen gas transmission rate (OTR) of BOPLA films coated with varying numbers of ALG/PEI layers and oxygen permeability of multilayer coatings (OP). (B) Oxygen permeability (OP) and water vapor permeability (WVP) as a function of number of layers of ALG and PEI deposited on BOPLA films.

strong interactions (electrostatic attractions and intermolecular H-bonding), this could also lead to reduced free volume for the interfacial polymers, which takes longer for oxygen molecules to travel through and causes them to have more interactions (Svagan et al., 2012). Sodium alginate has a T_g of 75 °C (Bertram & Bodmeier, 2006; Karidurganavar, Kittur, Kulkarni, & Ramesh, 2004), and PEI has a T_g of −26 °C (Yang et al., 2011). The LBL coating of ALG/PEI is higher than the linear additive combination of T_g of neat polymer, indicating that the strong attractions and interpenetrating network can also restrain the polymer chains and further decrease the mobility of each polymer (Yang et al., 2011). A schematic illustration of reduced free volume in highly interdiffused ALG/PEI layers and O_2 diffusion path is shown in Fig. 5. The upper part of the figure shows the interpenetration of the two polymer network. The circles in the lower part represent reduced free volume that result from the compact polymer interpenetrating network. The reduced free volume may be only few nanometer and takes longer time for oxygen molecules to travel through (Erlat et al., 2004; Yang et al., 2011). This densely packed interpenetrating structure and reduced free volume are the source of high barrier properties in these films.

The WVP of the multilayer-coated BOPLA films and neat BOPLA evaluated at 38 ± 0.2 °C and 90% RH is shown in Fig. 4B. These

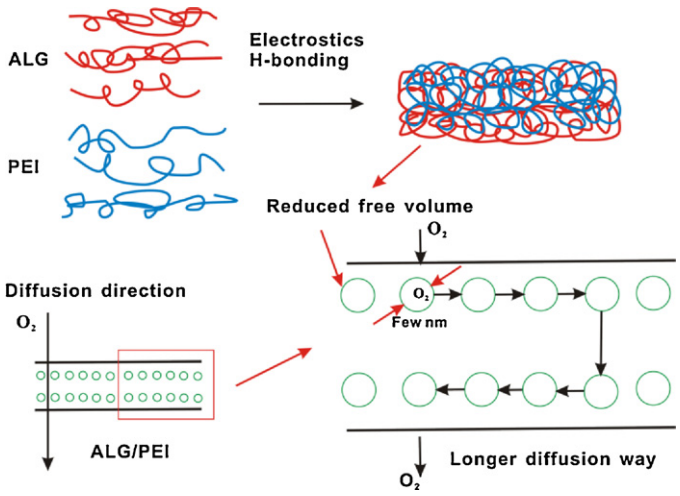

Fig. 5. Schematic of reduced free volume in highly interdiffused ALG/PEI layers and O_2 diffusion path.

data are calculated using Eq. (1). As the number of assembled layers increased, a slight decrease of WVP was detected, with a value of $2.44 \pm 0.01 \times 10^{-6}$ g cm/cm^2 s Pa for the neat BOPLA and $1.83 \pm 0.03 \times 10^{-6}$ g cm/cm^2 s Pa when 30 layers of ALG/PEI were applied. The lack of a larger improvement could be due to the hydrophilic nature of ALG and reduced polymer interaction at the interface due to the plasticizing effect of water, both of which could enhance the water vapor permeability (Hambleton, Debeaufort, Bonnotte, & Voilley, 2009; Kurek et al., 2012; Svagan et al., 2012). The chemical interaction between water and film materials that resulted in a volume expansion and the ultimately increase of free volume was found to have marked effects on water vapor permeation (Kaariainen et al., 2011; Erlat et al., 2004). This suggests that water vapor permeability should be further studied by changing the chemical composition of deposited polymer to reduce the chemical interaction of water and polymer and ultimately limiting the free volume to a smaller degree using LBL technique.

Table 1
The tensile properties of ALG/PEI coated BOPLA films.

Number of layer	Coating thickness (nm)	Tensile strength (MPa)	Breaking elongation (%)
0	0	136.15 ± 7.34	85.00 ± 1.66
10	1050 ± 225	136.29 ± 5.66	88.33 ± 1.67
20	2350 ± 475	135.78 ± 4.30	87.50 ± 2.48
30	3917 ± 625	137.38 ± 2.96	91.66 ± 2.51

3.2.2. Tensile properties

Mechanical properties of the obtained samples are summarized in Table 1, from which we can see that the obtained tensile strength

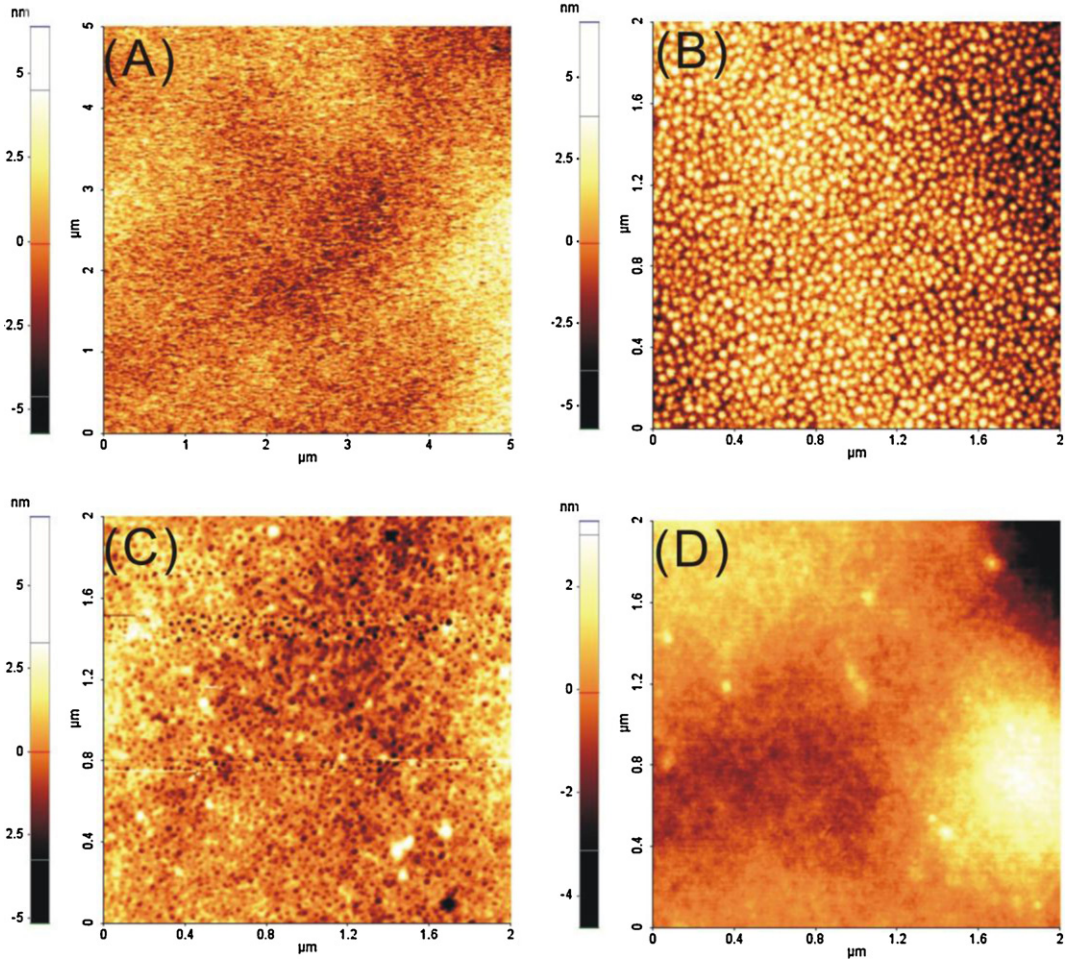

Fig. 6. AFM topography images of different BOPLA films: the BOPLA pure substrate (A), the PEI-modified BOPLA substrate (B), the ALG/CS multilayer assembled BOPLA substrate (C) and the ALG/PEI multilayer assembled BOPLA substrate (D).

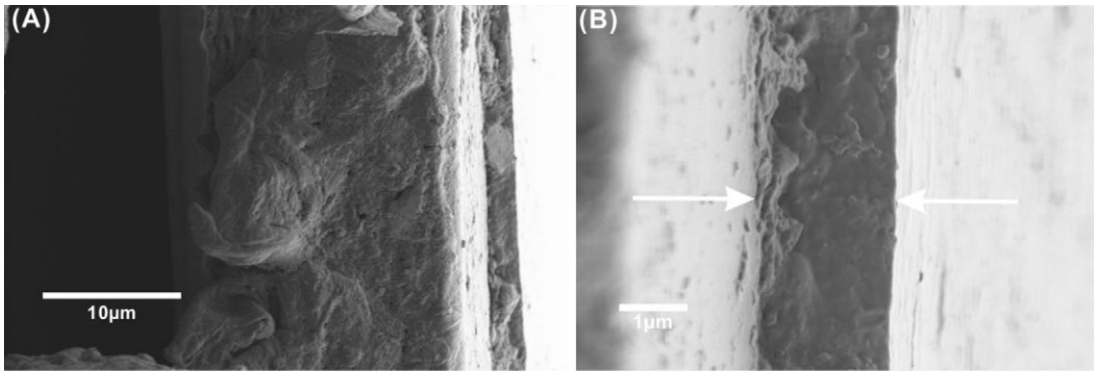

Fig. 7. FESEM images of cross-section at two different magnifications showing 30 layers of ALG and PEI on BOPLA films. The scale bars are 10 μm (A) and 1 μm (B).

and breaking elongation of pure BOPLA film are about 136 MPa and 85%, respectively. They are much higher than those of ordinary PLA films (63.67 MPa and 2.38%) reported previously (Cho et al., 2010). Specimens of the BOPLA films and of their multilayer coated BOPLA were evaluated by tensile testing, in order to investigate if the assembling process and thickness (see Fig. 3) of ALG/PEI would affect the mechanical properties of this biodegradable BOPLA substrate. From the results, the tensile strength and the elongation at break of multilayer-coated films are slightly improved with the number of layers increased from 0 to 30. This suggested that the coated layers are too thin to affect mechanical properties to change its initial mechanical properties. The mechanical properties of multilayer-coated BOPLA, being comparable to those of widely used plastic films, meet the requirements in the application of food packaging.

3.2.3. Transparency

A further advantage of using the LBL process to achieve all-polymer multilayer structures on BOPLA films is that the transparency (ranged from 88.3% to 91.7%) remains very close to that of the neat BOPLA film (92.6%).

3.3. Morphology of multilayer-coated BOPLA films

3.3.1. AFM images

Atomic force microscopy (AFM) surface images of BOPLA virgin substrate and the modified BOPLA substrates are shown in Fig. 6. The surface roughness of PEI-modified BOPLA film (1.8 nm) is higher than that of pure BOPLA film (1.3 nm) (Fig. 6A and B), which were all calculated using a 20 μm × 20 μm area. The surface of BOPLA virgin film shows an even topography (Fig. 6A). However, the surface of the PEI-modified BOPLA film is covered by a layer of globular granule less than 50 nm (Fig. 6B), which may contribute to the lower compatibility of the BOPLA-PEI copolymer with the PLA matrix (Zhu, Ji, et al., 2003; Zhu, Gao, et al., 2003). As to the coated BOPLA, a different morphology was shown from the BOPLA virgin substrate. The surface roughness of ALG/PEI (5.4 nm) is higher than that of ALG/CS (4.2 nm) (Fig. 6C and D). The AFM images clearly demonstrate the differences in surface coverage of the ALG associated with the different strategies, that is, a higher surface coverage of ALG associated with the ALG/PEI multilayer buildup (Aulin, Johansson, Wagberg, & Lindstrom, 2010). The more illegible image of multilayer modified BOPLA films than those of PEI modified BOPLA film is presumably linked to the charge overcompensation during the adsorption step (Zhu, Ji, et al., 2003; Zhu, Gao, et al., 2003). The ALG/CS modified BOPLA film surface exhibits large amounts of defects in few nanometer, which can be reflected by surface roughness. Compared with the pure BOPLA film, the OTR of ALG/CS modified BOPLA is little decreased. In contrast, the ALG/PEI modified BOPLA film (Fig. 6D) has a compact structure and its OTR is decreased greatly. It may attribute to the extended (thinner) polymer chain of CS due to its rigidity and partial crystallinity, which is difficult for ALG/CS to form compactly interpenetrated structure (Ogura, Kanamoto, Itoh, Miyashiro, & Tanaka, 1980; Podsiadlo et al., 2007; Tanigawa, Miyoshi, & Sakurai, 2008). On the contrary, the ALG/PEI modified BOPLA substrate (Fig. 6D) shows a more interdiffused morphology resulting a compact coil structure. Consequently, the free volume between the polymers is reduced (Yang et al., 2011).

3.3.2. Field emission scanning electron microscope (FESEM)

The FESEM photomicrographs of cross sections of 30 layers of ALG/PEI deposited on a BOPLA film at two different magnifications are shown in Fig. 7. The dense structure of the cross-section agrees with AFM measurements (Fig. 6). In Fig. 7B, particularly, the homogeneity structure without any obvious border can be seen similar to the structures previously observed (Yang et al., 2011). The densely packed structures of these images suggest a high level of interdiffusion between ALG and PEI that eliminates the boundaries between each layer. The thickness of the multilayer coating is estimated to be 1900 nm on average.

4. Conclusions

Contact angle and UV–vis absorbance measurements showed that multilayer bio-based polymer coating can be successfully constructed on BOPLA films using LBL technique. The resulting multilayer-coated BOPLA films showed significantly increased oxygen barrier properties as well as high optical clarity and tensile properties. Oxygen permeability of 30 layer ALG/PEI coating is the lowest ever reported for a biodegradable all-polymer LBL assembly (4.8×10^{-18} cm^3 cm/(cm^2 s Pa)) at a thickness of just 1.9 μm. FESEM images showed homogeneous and compact cross sections of the ALG/PEI modified BOPLA film, which suggested a densely interpenetrating network of ALG and PEI. The superior oxygen barrier provided by the multilayer ALG/PEI coating may be attributed to the reduced free volume created by interpenetrating network and hydrogen bonding. In contrast with the oxygen barrier effect, the WVP was reduced by only 25% when 30 layers were applied. That may be attributed to that the mechanism of water vapor permeation is more complicated.

In this work, it has been shown that the polysaccharides contained multilayer-coated biodegradable BOPLA films are considered highly promising for the future food packaging applications with super oxygen barrier properties. This study lays the foundation for further preparing of biopolymer-coated films with both higher oxygen and water vapor barrier that are needed for food packaging applications.

References

Aulin, C., Johansson, E., Wagberg, L., & Lindstrom, T. (2010). Self-organized films from cellulose I nanofibrils using the layer-by-layer technique. *Biomacromolecules*, *11*(4), 872–882.

Bang, G., & Kim, S. W. (2012). Biodegradable poly(lactic acid)-based hybrid coating materials for food packaging films with gas barrier properties. *Journal of Industrial and Engineering Chemistry*, *18*(3), 1063–1068.

Bertram, U., & Bodmeier, R. (2006). In situ gelling, bioadhesive nasal inserts for extended drug delivery: In vitro characterization of a new nasal dosage form. *European Journal of Pharmaceutical Sciences*, *27*(1), 62–71.

Carneiro-Da-Cunha, M. G., Cerqueira, M. A., Souza, B., Carvalhoc, S., Quintas, M., Teixeira, J. A., et al. (2010). Physical and thermal properties of a chitosan/alginate nanolayered PET film. *Carbohydrate Polymers*, *82*(1), 153–159.

Cho, S. W., Gallstedt, M., & Hedenqvist, M. S. (2010). Properties of wheat gluten/poly(lactic acid) laminates. *Journal of Agricultural and Food Chemistry*, *58*(12), 7344–7350.

De Mesquita, J. P., Donnici, C. L., & Pereira, F. V. (2010). Biobased nanocomposites from layer-by-layer assembly of cellulose nanowhiskers with chitosan. *Biomacromolecules*, *11*(2), 473–480.

Delpouve, N., Stoclet, G., Saiter, A., Dargent, E., & Marais, S. (2012). Water barrier properties in biaxially drawn poly(lactic acid) films. *Journal of Physical Chemistry B*, *116*(15), 4615–4625.

Dvoracek, C. M., Sukhonosova, G., Benedik, M. J., & Grunlan, J. C. (2009). Antimicrobial behavior of polyelectrolyte-surfactant thin film assemblies. *Langmuir*, *25*(17), 10322–10328.

Erlat, A. G., Henry, B. M., Grovenor, C. R. M., Briggs, A. G. D., Chater, R. J., & Tsukahara, Y. (2004). Mechanism of water vapor transport through PET/AlO_xN_y gas barrier films. *The Journal of Physical Chemistry B*, *108*(3), 883–890.

Fortunati, E., Armentano, I., Zhou, Q., Iannoni, A., Saino, E., Visai, L., et al. (2012). Multifunctional bionanocomposite films of poly(lactic acid), cellulose nanocrystals and silver nanoparticles. *Carbohydrate Polymers*, *87*(2), 1596–1605.

Guzman, E., Cavallo, J. A., Chulia-Jordan, R., Gomez, C., Strumia, M. C., Ortega, F., et al. (2011). pH-induced changes in the fabrication of multilayers of poly(acrylic acid) and chitosan: Fabrication, properties, and tests as a drug storage and delivery system. *Langmuir*, *27*(11), 6836–6845.

Hambleton, A., Debeaufort, F., Bonnotte, A., & Voilley, A. (2009). Influence of alginate emulsion-based films structure on its barrier properties and on the protection of microencapsulated aroma compound. *Food Hydrocolloids*, *23*(8), 2116–2124.

Iotti, M., Fabbri, P., Messori, M., Pilati, F., & Fava, P. (2009). Organic-inorganic hybrid coatings for the modification of barrier properties of poly(lactic acid) films for food packaging applications. *Journal of Polymers and the Environment*, *17*(1), 10–19.

Jamshidian, M., Tehrany, E. A., Imran, M., Akhtar, M. J., Cleymand, F., & Desobry, S. (2012). Structural, mechanical and barrier properties of active PLA-antioxidant films. *Journal of Food Engineering*, *110*(3), 380–389.

Jang, W. S., Rawson, I., & Grunlan, J. C. (2008). Layer-by-layer assembly of thin film oxygen barrier. *Thin Solid Films*, *516*(15), 4819–4825.

Kaariainen, T. O., Maydannik, P., Cameron, D. C., Lahtinen, K., Johansson, P., & Kuusipalo, J. (2011). Atomic layer deposition on polymer based flexible packaging materials: Growth characteristics and diffusion barrier properties. *Thin Solid Films*, *519*(10), 3146–3154.

Kariduraganavar, M. Y., Kittur, A. A., Kulkarni, S. S., & Ramesh, K. (2004). Development of novel pervaporation membranes for the separation of water–isopropanol mixtures using sodium alginate and NaY zeolite. *Journal of Membrane Science*, *238*(1), 165–175.

Koch, C.A., Akhave, J.R., & Bharadwaj, R.K. (2003). Layer by layer assembled nanocomposite barrier coatings. Google Patents.

Kurek, M., Brachais, C. H., Nguimjeu, C. M., Bonnotte, A., Voilley, A., Galić, K., et al. (2012). Structure and thermal properties of a chitosan coated polyethylene bilayer film. *Polymer Degradation and Stability*, *97*(8), 1232–1240.

Laufer, G., Kirkland, C., Cain, A. A., & Grunlan, J. C. (2012). Clay-chitosan nanobrick walls: Completely renewable gas barrier and flame-retardant nanocoatings. *ACS Applied Materials and Interfaces*, *4*(3), 1643–1649.

Lawrie, G., Keen, I., Drew, B., Chandler-Temple, A., Rintoul, L., Fredericks, P., et al. (2007). Interactions between alginate and chitosan biopolymers characterized using FTIR and XPS. *Biomacromolecules*, *8*(8), 2533–2541.

Li, Y. C., Schulz, J., Mannen, S., Delhom, C., Condon, B., Chang, S., et al. (2010). Flame retardant behavior of polyelectrolyte-clay thin film assemblies on cotton fabric. *ACS Nano*, *4*(6), 3325–3337.

Liu, A. D., & Berglund, L. A. (2012). Clay nanopaper composites of nacre-like structure based on montmorrilonite and cellulose nanofibers: Improvements due to chitosan addition. *Carbohydrate Polymers*, *87*(1), 53–60.

Marais, A., Kochumalayil, J. J., Nilsson, C., Fogelstrom, L., & Gamstedt, E. K. (2012). Toward an alternative compatibilizer for PLA/cellulose composites: Grafting of xyloglucan with PLA. *Carbohydrate Polymers*, *89*(4), 1038–1043.

Nuraje, N., Asmatulu, R., Cohen, R. E., & Rubner, M. F. (2011). Durable antifog films from layer-by-layer molecularly blended hydrophilic polysaccharides. *Langmuir*, *27*(2), 782–791.

Ogura, K., Kanamoto, T., Itoh, M., Miyashiro, H., & Tanaka, K. (1980). Dynamic mechanical behavior of chitin and chitosan. *Polymer Bulletin*, *2*(5), 301–304.

Park, S. H., Lee, H. S., Choi, J. H., Jeong, C. M., Sung, M. H., & Park, H. J. (2012). Improvements in barrier properties of poly(lactic acid) films coated with chitosan or chitosan/clay nanocomposite. *Journal of Applied Polymer Science*, *1251*, 675–680.

Picard, E., Espuche, E., & Fulchiron, R. (2011). Effect of an organo-modified montmorillonite on PLA crystallization and gas barrier properties. *Applied Clay Science*, *53*(1), 58–65.

Podsiadlo, P., Tang, Z., Shim, B. S., & Kotov, N. A. (2007). Counterintuitive effect of molecular strength and role of molecular rigidity on mechanical properties of layer-by-layer assembled nanocomposites. *Nano Letters*, *7*(5), 1224–1231.

Priolo, M. A., Gamboa, D., Holder, K. M., & Grunlan, J. C. (2010). Super gas barrier of transparent polymer-clay multi layer ultrathin films. *Nano Letters*, *10*(12), 4970–4974.

Priolo, M. A., Gamboa, D., & Grunlan, J. C. (2010). Transparent clay-polymer nano brick wall assemblies with tailorable oxygen barrier. *ACS Applied Materials and Interfaces*, *2*(1), 312–320.

Priolo, M. A., Holder, K. M., Gamboa, D., & Grunlan, J. C. (2011). Influence of clay concentration on the gas barrier of clay–polymer nanobrick wall thin film assemblies. *Langmuir*, *27*(19), 12106–12114.

Rhim, J. W., Hong, S. I., & Ha, C. S. (2009). Tensile, water vapor barrier and antimicrobial properties of PLA/nanoclay composite films. *LWT Food Science and Technology*, *42*(2), 612–617.

Richert, L., Lavalle, P., Payan, E., Shu, X. Z., Prestwich, G. D., Stoltz, J. F., et al. (2004). Layer by layer buildup of polysaccharide films: Physical chemistry and cellular adhesion aspects. *Langmuir*, *20*(2), 448–458.

Roberts, A. P., Henry, B. M., Sutton, A. P., Grovenor, C., Briggs, G., Miyamoto, T., et al. (2002). Gas permeation in silicon-oxide/polymer (SiO_x/PET) barrier films: Role of the oxide lattice, nano-defects and macro-defects. *Journal of Membrane Science*, *208*(1), 75–88.

Rossier-Miranda, F. J., Schroen, K., & Boom, R. (2010). Mechanical characterization and pH response of fibril-reinforced microcapsules prepared by layer-by-layer adsorption. *Langmuir*, *26*(24), 19106–19113.

Sanchez-Garcia, M. D., & Lagaron, J. M. (2010). On the use of plant cellulose nanowhiskers to enhance the barrier properties of polylactic acid. *Cellulose*, *17*(5), 987–1004.

Sui, L., Huang, L., Podsiadlo, P., Kotov, N. A., & Kieffer, J. (2010). Brillouin light scattering investigation of the mechanical properties of layer-by-layer assembled cellulose nanocrystal films. *Macromolecules*, *43*(22), 9541–9548.

Svagan, A. J., Akesson, A., Cardenas, M., Bulut, S., Knudsen, J. C., Risbo, J., et al. (2012). Transparent films based on PLA and montmorillonite with tunable oxygen barrier properties. *Biomacromolecules*, *13*(2), 397–405.

Tanigawa, J., Miyoshi, N., & Sakurai, K. (2008). Characterization of chitosan/citrate and chitosan/acetate films and applications for wound healing. *Journal of Applied Polymer Science*, *110*(1), 608–615.

Vartiainen, J., Tammelin, T., Pere, J., Tapper, U., & Harlin, A. (2010). Biohybrid barrier films from fluidized pectin and nanoclay. *Carbohydrate Polymers*, *82*(3), 989–996.

Wasikiewicz, J. M., Yoshii, F., Nagasawa, N., Wach, R. A., & Mitomo, H. (2005). Degradation of chitosan and sodium alginate by gamma radiation, sonochemical and ultraviolet methods. *Radiation Physics and Chemistry*, *73*(5), 287–295.

Xie, Y. L., Wang, M. J., & Yao, S. J. (2009). Preparation and characterization of biocompatible microcapsules of sodium cellulose sulfate/chitosan by means of layer-by-layer self-assembly. *Langmuir*, *25*(16), 8999–9005.

Yang, Y. H., Haile, M., Park, Y. T., Malek, F. A., & Grunlan, J. C. (2011). Super gas barrier of all-polymer multilayer thin films. *Macromolecules*, *44*(6), 1450–1459.

Yu, H. Y., Qin, Z. Y., Liu, Y. N., Chen, L., Liu, N., & Zhou, Z. (2012). Simultaneous improvement of mechanical properties and thermal stability of bacterial polyester by cellulose nanocrystals. *Carbohydrate Polymers*, *89*(3), 971–978.

Zhang, J., & Peppas, N. A. (2000). Synthesis and characterization of pH-and temperature-sensitive poly (methacrylic acid)/poly (N-isopropylacrylamide) interpenetrating polymeric networks. *Macromolecules*, *33*(1), 102–107.

Zhu, H., Ji, J., Tan, Q., Barbosa, M. A., & Shen, J. (2003). Surface engineering of poly(DL-lactide) via electrostatic self-assembly of extracellular matrix-like molecules. *Biomacromolecules*, *4*(2), 378–386.

Zhu, H., Ji, J., & Shen, J. (2004). Construction of multilayer coating onto poly(DL-lactide) to promote cytocompatibility. *Biomaterials*, *25*(1), 109–117.

Zhu, Y., Gao, C., He, T., Liu, X., & Shen, J. (2003). Layer-by-layer assembly to modify poly(L-lactic acid) surface toward improving its cytocompatibility to human endothelial cells. *Biomacromolecules*, *4*(2), 446–452.